Acoustic Measurement of Lubricant Film Thickness Distribution in Ball Bearings

Authors and Addresses:

Jie Zhang[1], Bruce W. Drinkwater[1] and Rob S. Dwyer-Joyce[2]

[1]Department of Mechanical Engineering, University Walk,

University of Bristol, Bristol BS8 1TR, UK

[2] Department of Mechanical Engineering, Mappin Street,

University of Sheffield, Sheffield S1 3JD, UK

SHORT TITLE:

Acoustic measurement of ball bearing oil film thickness

PACS NOS:

43.58.Gp Reflection, refraction, scattering of elastic and poroelastic waves

KEYWORDS:

ultrasound, thickness measurement, lubricant film, spring model

ABSTRACT

An oil-film thickness monitoring system capable of providing early warning of lubrication failure in rolling element bearings has been developed. The system is used to measure the lubricant-film thickness in a conventional deep groove ball bearing (shaft diameter 80 mm, ball diameter 12.7 mm). The measurement system comprises a high frequency (50 MHz centre frequency) broadband ultrasonic focused transducer mounted on the static outer raceway of the bearing. Typically the lubricant-films in rolling element bearings are between 0.1 – 1.0 μm in thickness and so are significantly smaller than the ultrasonic wavelength (120 μm in steel at 50 MHz). A quasi-static spring model is used to calculate oil-film thickness from the measured reflection coefficient data. As the lubricated 'contact' ellipse, has a minor axis of the order of 100 μm an accurate triggering system has been developed to enable multiple reflection coefficient measurements to be made as the contact ellipse sweeps over the measurement location. Experiments are described in which the loading conditions and rotational speed are varied. Lubricant-film thicknesses distributions measured ultrasonically are described and are shown to agree well with the predictions from classical elastohydrodynamic (EHD) lubrication theory, particularly at high radial

loads and low rotary speeds. A range of parameters affecting the performance of the measurement, including transducer focal spot size, bulk modulus and transducer positioning and alignment, are discussed and the limits of operation of the measurement technique defined.

1. INTRODUCTION

Fluid film lubrication occurs when opposing bearing surfaces are completely separated by a lubricant film, typically an oil or grease, which reduces friction and wear and provides smooth running and a satisfactory life for machine elements. The consequences of either film failure or absence of a film are usually manifested by severe friction and wear [1] and eventual failure of the bearing. Monitoring of the condition of bearings is therefore of major interest to a range of industries particularly those in the aerospace, marine, power generation and process sectors. In industry bearing condition monitoring is currently achieved by the measurement of running temperature, vibration signals, or acoustic emission. The disadvantage of all these techniques is that they are measuring the effect of an already partially failed bearing. A typical failure scenario in the event of a loss of lubricant is; an elevated temperatures caused by contact of the bearing surfaces, followed by a collapse of the oil film, surface spalling or pitting, increased vibration and possible acoustic emission.

Measurement of the lubricant-film thickness provides a more direct and quantitative way of monitoring the performance of a bearing, before actual bearing damage occurs. However, this is a challenging measurement as typically the load is carried by an extremely thin oil film over a small lubricated region. For example in a 6016 ball bearing (shaft diameter 80 mm, ball diameter 12.7 mm) the contact ellipse is 0.3 x 3 mm under typical (15 kN) operating load, and the oil film thickness is in the range 0.1-1.0 μm [2]. In this range, either electromagnetic or optical methods have been used to measure the lubricant film thickness. However, these techniques suffer from serious drawbacks. The resistance [3] and capacitance methods [4,5] require either an insulated surface mounted sensor, or complete electrical isolation of the contact elements. These methods are generally limited to lubricant films above about 1 μm in thickness [6,7]. Optical interferometry [8] and optical fluoresence techniques [9] have also been used in test bearings but these require a transparent window though which to make the measurement. These requirements mean that both electromagnetic and optical methods are rarely used outside the laboratory.

Recently a number of workers have performed measurements of lubricant thickness using various ultrasonic techniques. Anderson et al [10] used the transmission and reflection of ultrasonic waves to monitor the collapse of oil-films in thin shaft seals. Dwyer-Joyce et al [11] and Zhang et al [12] used ultrasonic reflection coefficient measurements to monitor the lubricant-film thickness in thick film bearings such as journal bearings and thrust-pad bearings. In these bearings the lubricant film was in the range 1.0-20 μm and the film was constant with respect to the fixed transducer. The results were shown to agree well with models of the bearing performance. This paper takes the work a critical step forward and shows for the first time that ultrasound can be used to measure accurately the lubricant-film thickness distribution in rolling element bearings. The rolling element bearing application is considerably

more challenging than the previously published hydrodynamic applications as the contact patches are moving relative to the fixed transducer and the size of the contact and thickness of the lubricant in the contact are an order of magnitude lower. Furthermore, the use of the ultrasonic technique on rolling element bearings opens up a wide range of novel industrial applications.

2. BACKGROUND THEORY

2.1. Ultrasonic Reflection from an Oil Film

The structure of a rolling element bearing can be represented as a multi-layered system consisting of outer raceway-lubricant film-ball-lubricant film-inner raceway. When an ultrasonic pulse propagates through this structure, ultrasound will be reflected from all the interfaces within the system, including from the lubricant layer. If the thickness of the lubricant-layer is small in comparison with the ultrasonic wavelength it can be shown that the reflection of ultrasound from such a layer is governed only by its stiffness [12]. The normal stiffness of a fluid layer, K_N, is given by [10]:

$$K_N = \sqrt{\frac{B}{\rho}} \tag{1}$$

where B is the Bulk Modulus of the fluid (and $B = \rho c^2$), ρ and c the density and longitudinal wave speed of the fluid respectively. Assuming that the media either side of the layer have identical acoustic properties and that the wave is normally incident the lubricant-film thickness can then be extracted from the well known quasi-static spring model as:

$$h = \frac{B}{\pi f z}\sqrt{\frac{|R(f)|^2}{1-|R(f)|^2}} \tag{2}$$

where z is the acoustic impedance of the media surrounding the lubricant film, $R(f)$ is the amplitude of the measured reflection coefficient which is a function of the ultrasonic frequency, f. In general the reflection coefficient is measured by comparing the signal reflected from the interface of interest to that from a known reference interface:

$$R(f) = \frac{A_m(f)}{A_{ref}(f)} R_{ref} \tag{3}$$

where, $A_m(f)$ is the amplitude of the signal reflected from the lubricant-film layer, $A_{ref}(f)$ is the amplitude of the reference signal and R_{ref} is the reflection coefficient of the reference interface. The reflection coefficient calculated from equation 3 can then be used in equation 2 to extract the lubricant film thickness assuming all other material constants, acoustic properties and the reference reflection coefficient are known.

Figure 1 shows a plot of the steel-oil-steel reflection coefficient over a wide range of frequency-thickness products where frequency-thickness is plotted to generalise the results. This was calculated using a three layer continuum model [13] with the material property data shown in Table 1. Figure 1 also indicates the region over which the quasi-static spring model can be applied. In their recent paper Zhang et al [11] analysed the error inherent in the use of the quasi-static spring model to calculate layer thickness from reflection coefficients. For example, they suggested that thickness errors of less than 2 % will result if equation 2 is used below the first resonance and for $0.1<R<0.95$ when standard derivation of R is 1%. These limits are shown in Figure 1 as $1.3<hf<38$ MHz.μm. For the 50 MHz transducer with 30-75 MHz bandwidth (measured at the –6 dB points) used in this paper this equates to a lubricant-film thickness range of 0.02 – 1.3 μm. It is the aim of this paper to demonstrate that such a measurement can be realised and that this can be performed on a rotating element bearing operating under typical conditions.

2.2. Oil Film Formation in a Ball Bearing

The geometry of the contact that forms when a ball is pressed onto a closely conforming raceway groove can be calculated from the applied load, P [1]. The contact area is elliptical in shape with the major (r_a) and minor (r_b) semi-contact radii given by:

$$r_a = \left(\frac{6k^2 \varepsilon P R'}{\pi E'} \right)^{1/3} \qquad r_b = \left(\frac{6 \varepsilon P R'}{\pi k E'} \right)^{1/3} \tag{5}$$

where k and ε are a measure of the shape of the contact ellipse obtained from look-up tables [1]. E' is the reduced elastic modulus and R' is the reduced radius of curvature given by:

$$\frac{1}{E'} = \frac{1}{2}\left[\frac{1-\nu_a^2}{E_a} + \frac{1-\nu_b^2}{E_b} \right]$$

$$\frac{1}{R'} = \frac{1}{R_{ax}} + \frac{1}{R_{bx}} + \frac{1}{R_{ay}} + \frac{1}{R_{by}}$$

where E refers to elastic modulus, and ν refers to Poisson's ratio. The subscripts a and b refer to the two rolling elements (i.e. the ball and the raceway), and R_x and R_y refer to the radii of curvature in the x and y directions respectively.

The geometry of the ball and raceway is such that the major semi-contact width r_a is around ten times the minor semi-contact width r_b. (shown schematically in figure 5). The ball sweeps across the raceway in the x-direction so ultrasonic measurements are made across the minor axis of this ellipse minor axis. The pressure distribution over the elliptical region is given by [1]:

$$p = p_0 \sqrt{1 - \left(\frac{x}{r_b}\right)^2 - \left(\frac{y}{r_a}\right)^2} \qquad (6)$$

where p_0 is the maximum contact pressure, that occurs at the centre of the ellipse. The load on the ball is not the same as that on the whole bearing, because several balls are in contact with the raceways at any instant. The load on the maximum loaded ball, P directly opposite the point of application of the bearing load is given by [Jie ref Harris book]:

$$P = \frac{5W}{n} \qquad (XX)$$

where W is the radial load on the whole bearing and n is the number of the balls in the compliment. The mean and peak contact pressures are then given by:

$$p_m = \frac{P}{\pi r_a r_b} \text{ and } p_0 = \frac{3P}{2\pi r_a r_b} \qquad (XX)$$

For a ball bearing, operating in the elastohydrodynamic lubrication regime, the lubricant-film thickness can be estimated from the numerically derived regression equations of Dowson & Higginson [1,14]. They showed that the central film thickness, h_c, can be expressed as:

$$\frac{h_c}{R'} = 2.69\left(\frac{U\eta_0}{E'R'}\right)^{0.67}\left(\alpha E'\right)^{0.53}\left(\frac{P}{E'R'^2}\right)^{-0.067}\left(1 - 0.61e^{-0.73k}\right) \qquad (4)$$

where, U is the mean surface speed, η_0 is the lubricant viscosity at the contact entry, and α is the pressure-viscosity coefficient.

It is well know that the mechanical and acoustic properties of mineral oils vary with both temperature and pressure. In this experiment the measurements were taken over a short period of time (typically less than 30 mins). Between measurements the system was allowed to cool to room temperature. During this time the temperature of the bearing was measured and found to vary by 2ºC for the highest load and speed case. This temperature variation will have a small affect on the film thickness and acoustic properties and so this effect is neglected in the rest of this paper.

However, contact pressures in the ball bearing contacts are very high, and this has the effect of increasing both the density and the bulk modulus of the lubricant. Jacobson and Vinet [17] developed a model for this bulk modulus variation. They give an equation of state to describe the behaviour of the lubricant under pressure, p:

$$p = \frac{3B_0}{x^2}(1 - x)\,\mathrm{e}^{\eta(1-x)} \qquad (9)$$

and the bulk modulus under pressure is given by:

$$B = \frac{B_0}{x^2}\left[2 + (\eta - 1)x - \eta x^2\right]e^{\eta(1-x)} \tag{10}$$

where B_0 is the bulk modulus at zero pressure, η is a lubricant specific parameter, and x is a function of the relative compression:

$$x = \sqrt[3]{\frac{\rho_o}{\rho_p}} \tag{11}$$

where ρ_0 is the density at zero pressure, and ρ_p at pressure p. The parameter, η is determined empirically from tests on lubricants in high pressure cells (up to 2.2 GPa). Because of the experimental complexities this data is scare; in this paper we use data available for an oil of a similar generic type to Shell T68. Table 2 shows the bulk modulus determined at three contact pressures.

The parameters used in equations 4 and 5 are also shown in Table 2. In this paper, the lubricant-film thicknesses were calculated from reflection coefficient measurements using a quasi-static spring model (equation 1), and compared with the Dowson and Higginson theoretical film thickness (equations 4 and 5).

3. BALL BEARING EXPERIMENTAL APPARATUS

Experimental apparatus capable of accurately measuring the ultrasonic reflection coefficient from a lubricant film in the 6016 bearing system is shown in Figure 2(a). The bearing rig consisted of a rotating shaft of 80 mm diameter supported on four 6016 ball bearings and ultrasonic transmit-receive instrumentation. As shown in Figure 2(a), bearings 1 and 4 were fitted to the ends of the shaft and fixed into rigid housings. Radial loads were applied to the shaft though bearings 2 and 3. The load was applied vertically downwards by an arrangement of springs. This meant that in bearings 1 and 4 the ball at the top of the raceway was the most heavily loaded. The rotary shaft speed was controlled by a 7.5 Watt (is this right?? 7.5W only? Surely kW) motor in the range 100-2900 rpm. The bearing was lubricated with Shell T68 mineral oil via a total loss gravity feed system. An optical sensor was used, both to allow accurate triggering of the ultrasonic instrumentation and to measure shaft speed. This was triggered of reflective tape attached to the ball cage (which rotates at half the shaft speed). Bearing 1 was instrumented with the ultrasonic measurement system. Figure 2(b) shows the ultrasonic measurement system in more detail. A focused, longitudinal wave piezoelectric ultrasonic transducer was mounted in the housing such that it was normal to the top surface of the outer raceway. This transducer, detailed in Table 1, acted as both an emitter and receiver (pulse-echo mode), and had a centre frequency of 50 MHz, an active element diameter of 5 mm and a focal length in water of 23 mm. This equates to a theoretical focal spot size (defined at –6dB down from the maximum) in the plane of the lubricant film of 146 μm at the centre frequency. This spot size defines the spatial resolution of the measurement system. The transducer was selected to be as high frequency as possible, whilst still able to operate in a regime where material attenuation was acceptable. The transducer was connected to an ultrasonic pulser-receiver (Panametrics 5072PR) with bandwidth 5-200 MHz was used to excite this ultrasonic transducer, receive and amplify the

reflected signals which were then passed to a digital scope (sample frequency 250 MHz) and PC for storage and analysis.

The reflective tape attached to the bearing cage is also shown in Figure 2(b). When this tape passed the optical sensor it generated a positive pulse. This pulse was used to trigger a signal generator (Angilent 33220A). After the addition of an adjustable delay the signal generator then triggered the pulser-receiver at its maximum pulse repetition frequency, which was 20 kHz. By triggering in this way, a number of ultrasonic pulses were able interrogate the lubricated 'contact' region as it passed under the transducer. Because of memory limitations in the oscilloscope, only 80 reflected pulses could be stored in the oscilloscope at any time and hence this is the maximum number of measurement points. The number of measurement points was governed by a combination of the pulser-receiver repetition rate and the speed at which the balls in bearing passed the transducer. The delay between the optical trigger and the triggering of the pulser-receiver was adjusted by knowledge of the shaft speed and the distance between the trigger point and the focal spot of the transducer.

In order to calculate reflection coefficient it is necessary to obtain a reference reflection from a known interface. The apparatus was used to obtain a steel-air reflection before lubricant was introduced. The steel-air reflection coefficient is known to be 0.99998. Using this reference all measured reflections were converted to reflection coefficient via equation 3 and this analysis was performed in the frequency domain.

4. RESULTS

4.1 Central Thickness

Figure 3 shows the experimentally measured reflection coefficients for various shaft speeds from 106-506 rpm and a test bearing radial load of 15 kN. Data is recorded as the ball passes under the measurement location and so a reflection coefficient profile is created. It can be seen that the reflection coefficient falls to a minimum at the centre of the lubricated contact region and then rises again. Also, at the centre of the lubricated contact it can be seen that the reflection coefficient decreases with increasing shaft speed.

The reflection coefficient recorded when the ball is immediately below the transducer (i.e. the centre of the contact x=0 in figure 3) has been used to calculate the oil film thickness using equation 2. Figure 4 shows a comparison between this measured film-thickness and the theoretical lubricant-film thickness (equation 4) for a range of different operation conditions. Different points for the same combination of speed and load represent separate readings and indicate the scatter in the measurement. For a given shaft speed, the experimental thickness decreases with increasing radial load. These experimentally measured trends are in reasonable agreement with those predicted by the elastohydrodynamic theory. It is also worth noting that there is better quantitative agreement at high loads and low speeds. Possible reasons for the discrepancy observed in Figure 4 are explored in detail in Section 5.

4.2 Thickness Distribution

The measured reflection reflection coefficient profiles shown in Figure 3 are now used to calculate the oil film thickness distribution across the contact (again using equation 2). However, it is necessary to first account for variation in lubricant bulk modulus as it changes over the contact width. The pressure distribution across the contact width (in the *x*-direction) is obtained from equation 6. It is assumed that the measured reflection results are recorded along the ellipse axis *y*=0. The bulk modulus along this line is then determined using equations 9, 10, and 11.

Figure 5(b) shows this bulk modulus distribution for several of applied loads. It is worth noting that from equation 2, uncertainties in bulk modulus will translate directly in to uncertainties in measure lubricant-film thickness.

Figure 5(c) shows lubricant-film thicknesses distribution extracted from the reflection coefficient profiles (figure 3) using the bulk modulus distribution shown in Figure 5(b). It can be seen that this measured thickness distribution is characterised by the 10-80 reflected signals (what does 10-80 mean?), depending on the shaft speed. Also shown in Figure 5(c) is the theoretical thickness distribution (assuming the central film thickness calculation is valid across the whole contact). It can be seen that there is good agreement at the centre of the lubricated contact and that elsewhere the agreement is less good. In Section 5 we seek to explain the observed shape of this thickness distribution as well as discuss a range of measurement issues that may lead to uncertainties in the measured thickness.

5. DISCUSSION

In this section the acoustic pressure distribution over the focal spot is used to explain the shape of the experimentally measured lubricant-film distribution. Errors in the reflection coefficient due to the orientation of the transducer with respect to the lubricated contact are discussed and quantified. The limits of operation of the technique are then discussed.

5.1 Effect of the transducer focal zone size

When focused on the lubricant film, the ultrasonic transducer measures an average reflection coefficient, weighted by the acoustic pressure distribution in the plane of the lubricant film. The acoustic pressure distribution in the focal plan of a circular transducer is given by [18]:

$$p(x) = \left| 2\,p_0 \left(\frac{\pi D x}{\lambda F} \right)^{-1} J_1 \left(\frac{\pi D x}{\lambda F} \right) \right| \qquad (7)$$

where p_0 is the centre acoustic pressure (set to unity to normalize the pressure distribution), F is the focal length, x radial distance from the central axis, D is the diameter of the active element, λ is the wavelength, and J_1 is the first-order Bessel function. The application of equation 7 to the transducer used in this work, detailed in Table 1 gives a theoretical focal spot width (measured at –6dB of the maximum

pressure) of 146 μm at 50 MHz. However, when this transducer was moved over a sharp edge its focal spot size was estimated as being 500 μm. This discrepancy is probably due to a combination of a slight roundness present on the sharp edge and a small underperformance of the transducer. Figure 6(a) shows the acoustic pressure distribution predicted for the transducer data shown in Table 1 as well as for a transducer with 300 μm and 500 μm spot sizes.

The acoustic pressure distribution can now be used to weight the reflection coefficient predicted via equations 4 and 2. The weighting procedure takes the following form:

$$R_w(x_i) = \frac{\int_{-\infty}^{\infty} p(x - x_i)R(x)dx}{\int_{-\infty}^{\infty} p(x)dx} \tag{8}$$

where, R and R_w are the unweighted and weighted reflection coefficients respectively and x_i refers to x position at which the weighted average is calculated.

Figure 6(b) shows the simulated measured lubricant film thickness based on equation 4 and the weighted version using the above equation 8 and then equation 2. From Figure 6(b) it can be seen that as the spot size increases, so the 'curvature' of the thickness distribution increases. It is also apparent that the form of the thickness distribution predicted in Figure 6(b) is similar to that measured experimentally and shown in Figure 5(c). It can also be seen that the central value of lubricant-film thickness shows close agreement with the 'theoretical' value as it is least affected by the focal spot size effect.

5.2 Effect of transducer orientation

As the ball bearing passes the measurement region the orientation of the lubricant film with respect to the transducer axis changes. The angle of this slope, θ, is shown in Figure 7(a) and can be expressed as:

$$\theta = \omega T = \omega N \Delta t \tag{9}$$

where ω is the angular velocity of the ball and T is the time since the ball was at top dead centre (TDC), i.e. directly below the central axis of the transducer. This can also be written in terms of the number of measurement points since TDC, N and the sampling interval, Δt (50 μs). Figure 7(b) shows how this angle increases with increasing the time from TDC. Also shown in Figure 7(b) are horizontal lines that show the maximum angle monitored within the contact patches generated at a number of different loads. The angular range from 0 (i.e. the contact patch is normal to the transducer axis) to these lines represents cases encountered in this paper. Ray tracing theory and angle-dependent spectral distortion (ASD) theory [19, 20] can be used to analyse the effect of this slope on the measured reflection coefficient. There are two points in considering this slope effect, the projection of the ultrasound ray on the radiator and the effective active zone in the radiator. The projection angle φ can be found from:

$$\varphi = \beta - \tan^{-1}\left(\frac{a}{F}\right) \tag{10}$$

where, $a = d_2 \tan 2\theta + d_1 \tan\beta$, β is the angle of the central reflected ray in the water which can be obtained from Snell's law and the other parameters are defined in Figure 7(a).

Figure 7(c) shows the geometries of the receiving zone of the transducer and the reflected ultrasonic beam projection. When the balls are at TDC the receiving area and reflected projection overlap exactly. At a given projected angle, the reflected signal is reduced by:

$$Q = 1 - \frac{4r^2 \cos^{-1}\left(\frac{a}{2r}\right) - \frac{a}{2}\sqrt{r^2 - \frac{a^2}{4}}}{\pi r^2}\cos\varphi \tag{11}$$

where, r is the radius of the active element. Figure 7(d) shows this as a relative error as a function of the angle of slope, θ. For example, if lubricant film thickness measurement accuracy of 2 % is required, the experimental data should be only captured when the angle of slope of the lubricated contact region is less than 0.2º. Note that this error will always happen at the edges of the lubricated contact region where the angle of slope is greatest. Also note that this effect will tend to cause a reduction in the measured reflection coefficient and hence an underestimate of the lubricant film thickness. This is also good confirmation that the measured central thicknesses is the least prone to error and therefore most suitable for comparison with theoretical values.

5.3 Limits of operation

At present, the measurement system is limited to a time interval of 50 μs by the maximum pulse repetition frequency (20 kHz) achievable by pulser-receiver. If this could be improved then the next limit would be due to the ultrasonic waves reverberating in the coupling water and the outer raceway and hence not decaying to zero before the next measurement. For the bearing and transducer configuration used in this paper this limit was estimated at 20 μs.

Figure 8 shows limits of operation for the current equipment and bearing geometry. Three regimes have been defined in this graph. When the bearing is operating at low radial load and high shaft speed a small, fast moving, lubricated contact is generated. If this is such that only one point can be measured per ball then this is indicated on Figure 8 as the poor operating regime. If the speed and load are such that the lubricated 'contact' region is larger than the spot size of the transducer and at least two measurement points can be obtained for each ball passage, this was classified as the acceptable operating regime. In the good operating regime, more than two reflected signals can be used to characterise each lubricated contact. In this paper all measurements presented have been from within the good operating regime. It is worth noting that an increase in the pulse repetition frequency, a reduction in the focal

spot size of the transducer, or an increased test bearing size, will result in an increase in the sizes of the good and acceptable measurements regimes.

6. CONCLUSIONS

Ultrasonic reflection coefficient measurements have been used to measure the lubricant-film thickness of a rotating element ball bearing (type 6016). Measurements of lubricant film thickness in the range 0.1-1.0 μm have been made and shown to be in good agreement with known elastohydrodynamic lubrication theory when the radial load was larger than 2.5 kN and the shaft speed was lower than 200 rpm. The ultrasonic transducer produces an 'averaging' effect, due to the focal spot size of the transducer and this was shown to explain the form of the measured lubricant film thickness distribution. In this way the focal spot size defines the spatial resolution of the measurement system. The measurement system was also shown to be limited by the maximum achievable pulse-repetition frequency. This determines the number of measurement points obtained across the lubricated contact. The performance of the experimental system demonstrates that this approach has the potential for condition monitoring of lubricant layers in industrial application.

ACKNOWLEDGEMENTS

This work has been funded by the UK Engineering and Physical Sciences Research Council.

REFERENCES

1. Stachowiak, G.W. and Batchelor, A.W., 2001, *Engineering Tribology* (Butterworth Heinemann).

2. Hamrock, B. J., Schmid, S. R., and Jacobson, B. O., 2004, *Fundamentals of Fluid Film Lubrication*, *Second Edition* (Marcel Dekker, Inc.).

3. El-Sisi, S. I. and Shawki, G. S. A., 1960, Measurement of oil-film thickness between disks by electrical conductivity, *Transactions of ASME: Journal of Basic Engineering,* **82**, 12-18.

4. Astridge, K. G. and Longfield, M. D., 1967, Capacitance measurement and oil film thickness in a large radius disc and ring machine, *Proceedings of the Institute of Mechanical Engineers,* **182**, 89-96.

5. Dyson, A., 1967, Investigation of the discharge-voltage method of measuring the thickness of oil films formed in a disc machine under conditions of elastohydrodynamic lubrication, *Proceedings of the Institute of Mechanical Engineers,* **181**, 633-645.

6. Ducu, D.O., Donahue, R.J., and Ghandhi, J.B., 2001, Design of capacitance probes for oil film thickness measurements between the piston ring and liner in internal combustion engines, *Journal of Engineering for Gas Turbines and Power*, **123**, 633-643.

7. Cameron, A. and Gohar, R., 1966, Theoretical and experimental studies of the oil film in lubricated point contact, *Proceedings of the Royal Society, London: Part A,* **291**, 520-536.

8. Richardson, D.A. and Borman, G. L., 1991, Using fibre optics and laser fluorescence for measuring thin oil films with applications to engines, *Society of Automotive Engineers, SAE Paper* 912388.

9. Anderson, W., Jarzynski, J. and Salant, R.F., 2000, Condition monitoring of mechanical seals: detection of film collapse using reflected ultrasonic waves, *Proceedings of the Institute of Mechanical Engineers: Part C*, **214**, 1187-1194.

10. Dwyer-Joyce, R.S., Drinkwater, B.W., and Donohoe, C.J., 2003, The measurement of lubricant-film thickness using ultrasound, *Proceedings of the Royal Society, London: Part A,* **459**, 957-976.

11. Zhang, J, Drinkwater B.W. and Dwyer-Joyce R.S., 2005, Calibration of the Ultrasonic Lubricant Film Thickness Measurement Technique, *Measurement Science and Technology*, in press.

12. Rokhlin, S.I. and Wang, Y.J., 1991, Analysis of boundary conditions for elastic wave interaction with an interface between two solids, *Journal of he Acoustical Society of America*, **89(2)**, 503-515.

13. Pialucha, T. and Cawley, P, 1994, The detection of thin embedded layers using normal incidence ultrasound, Ultrasonics, Vol. 32(6), pp. 431-440.

14. Dowson, D. and Higginson, G. R., 1977, *Elasto-Hydrodynamic Lubrication* (Pergamon Press).

17. Jacobson, B. O. and Vinet, P. A., 1987, Model For The Influence Of Pressure On The Bulk Modulus And The Influence Of Temperature On The Solidification Pressure For Liquid Lubricants, *Journal Of Tribology-Transactions Of The ASME*, **109**, 709-714.

18. Silk, M. G., 1984, *Ultrasonic Tansducers for Nondestructive Testing* (Adam Hilger Ltd).

19. Orofino, D. P. and Pedersen, P. C., 1992, Angle-Dependent Spectral Distortion For An Infinite Planar Fluid-Fluid Interface, *Journal Of The Acoustical Society Of America*, **92**, 2883-2899.

20. Orofino, D. P. and Pedersen, P. C., 1993, Evaluation Of Angle-Dependent Spectral Distortion For Infinite, Planar Elastic Media Via Angular Spectrum Decomposition, *Journal Of The Acoustical Society Of America*, **93**, 1235-1248.

LIST OF FIGURES

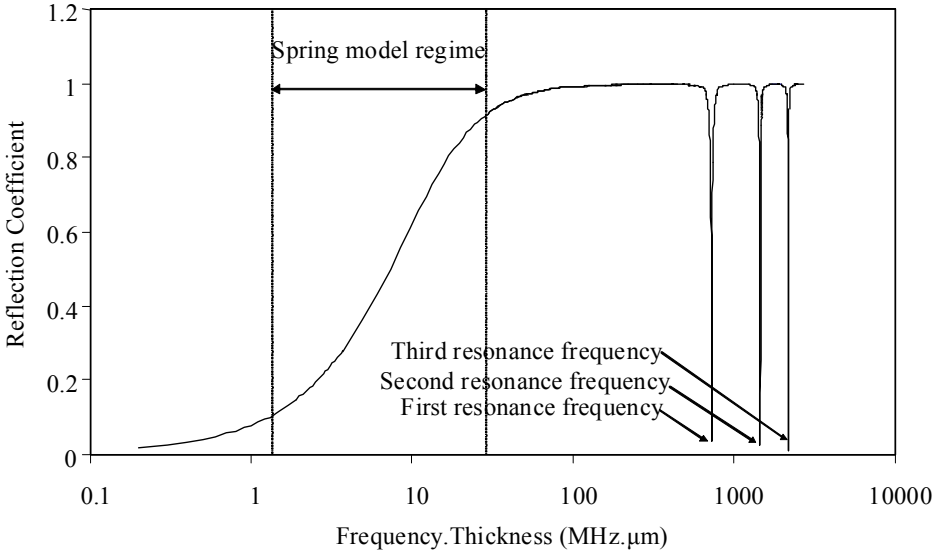

Figure 1. Predicted reflection coefficient spectrum for a layer of mineral oil between two steel half spaces.

Figure 1. Predicted reflection coefficient spectrum for a layer of mineral oil between two steel half spaces.

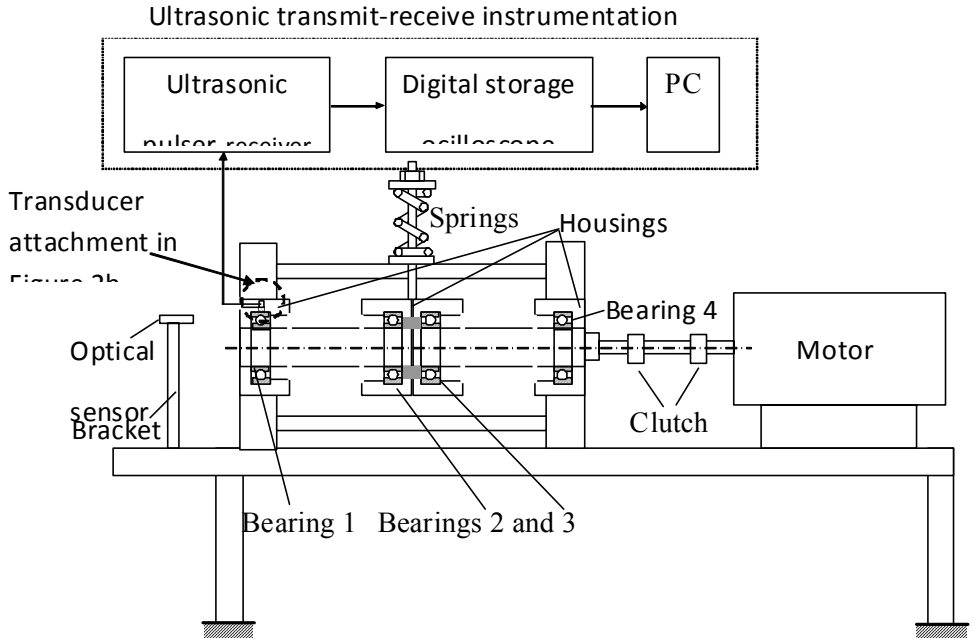

Figure 2(a). Schematic diagram of the experimental apparatus made up of four 6016 ball bearings.

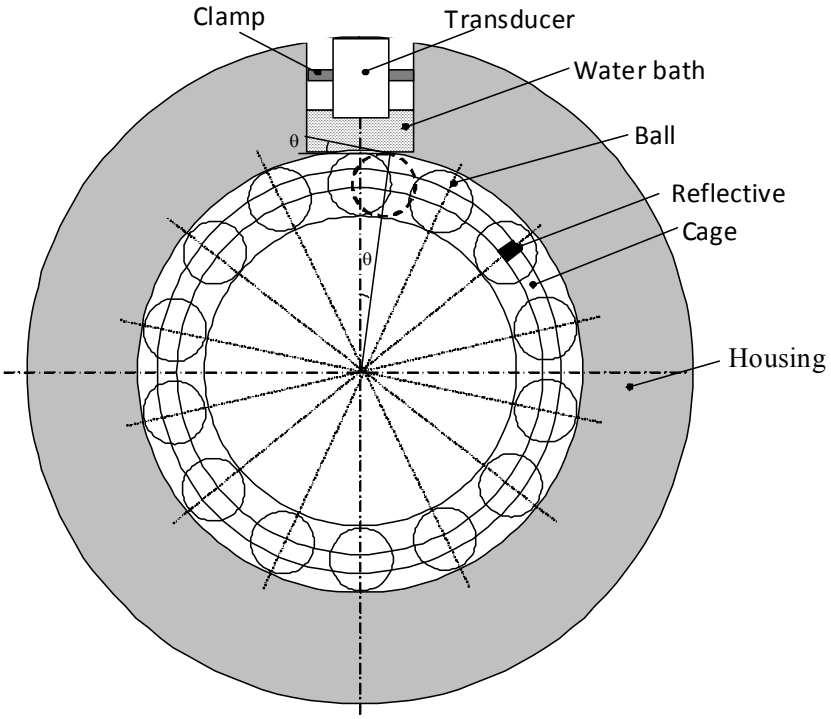

Figure 2(b). Transducer attachment.

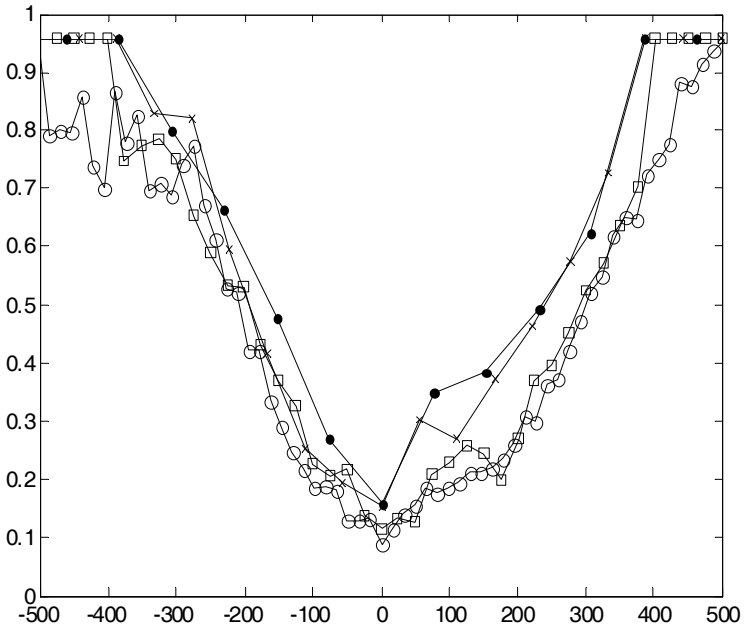

Figure 3. Reflection coefficient recorded for various shaft speeds at a radial load of 15 kN.

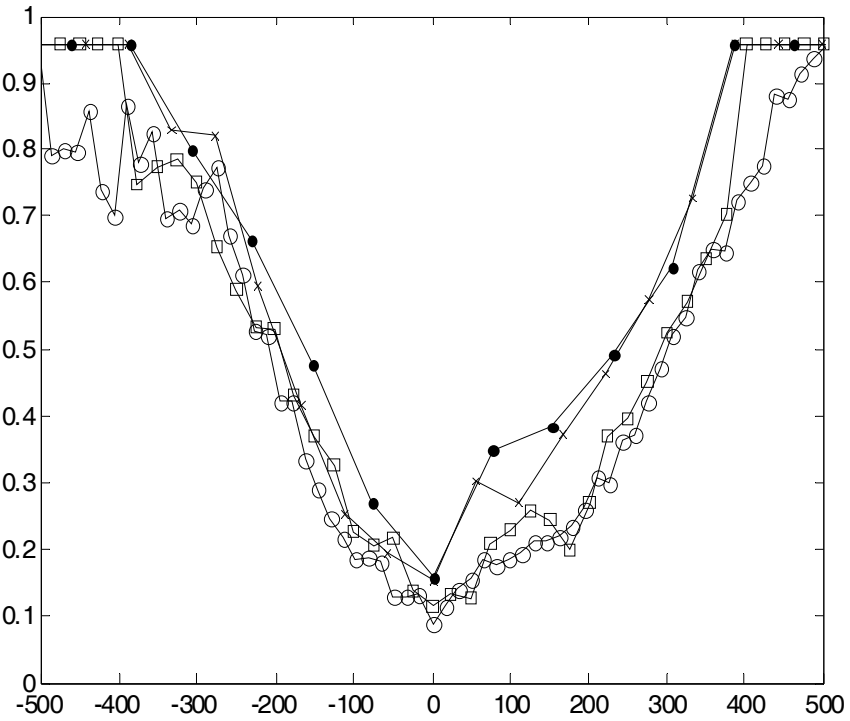

Figure 4. Comparison of lubricant-film thicknesses measured by an ultrasonic means with EHD theoretical solution at various radial load and shaft speeds.

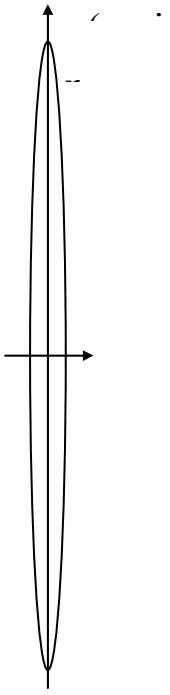

Figure 5(a). Schematic diagram of the lubricated contact region of the ball bearing.

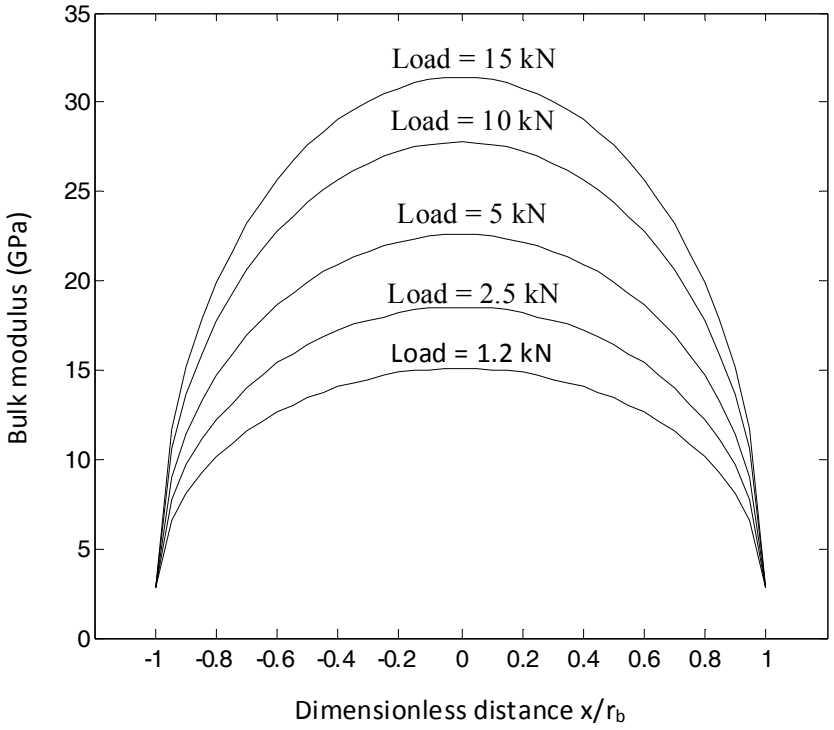

Figure 5(b). Bulk modulus distribution along the minor axis at various radial loads.

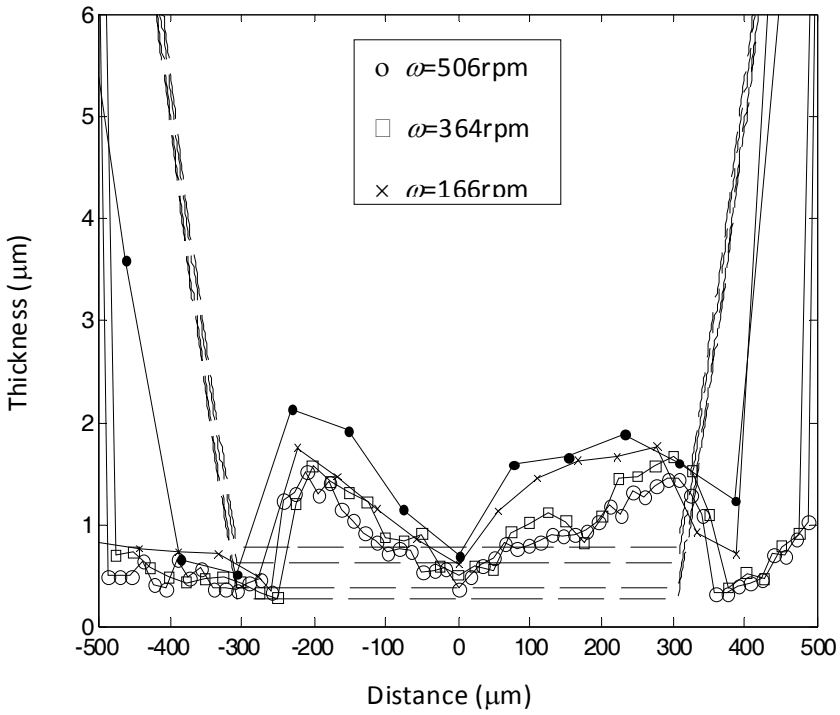

Figure 5(c). Measured oil film thickness recorded for various shaft speeds at a radial load of 15 kN. Results are compared with the theoretical thicknesses indicated by the dashed line.

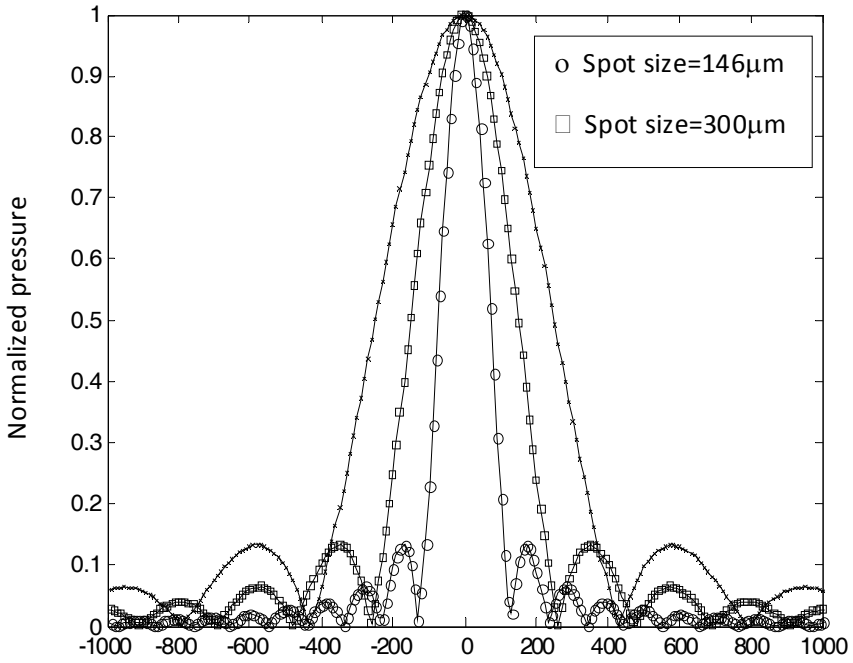

Figure 6(a). The acoustic pressure distribution at the focal plane for transducers with various spot sizes.

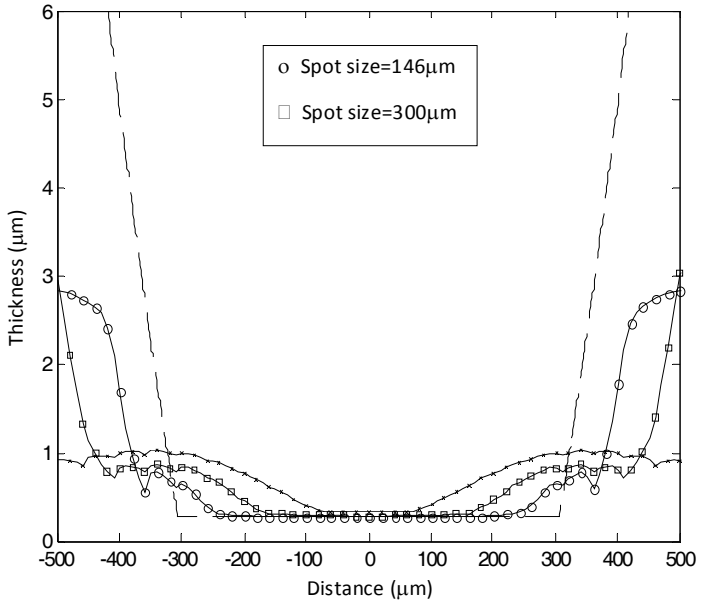

Figure 6(b). Lubricant-film thicknesses calculated by theory and using weighting function of acoustic pressure distribution at the focal plane. Results from various spot size are compared.

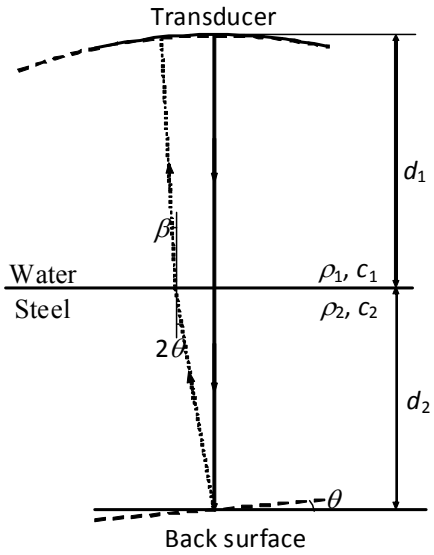

Figure 7(a). Comparison of the geometries of the reflected signal from a normal surface and a surface with a small slope.

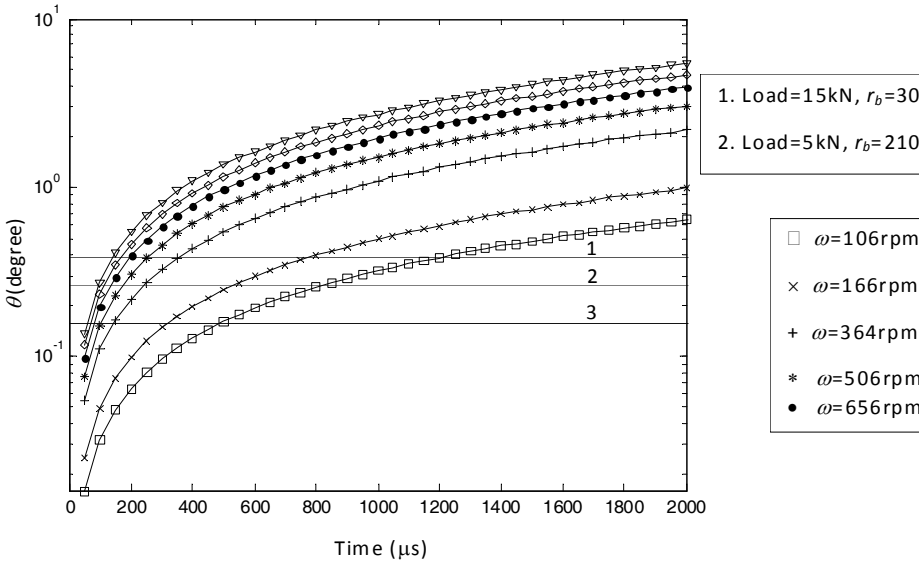

Figure 7(b). The angle of the slope of lubricated contact area versus the time from TDC. The horizontal lines for various loads indicate the maximum angle in the lubricated contact area.

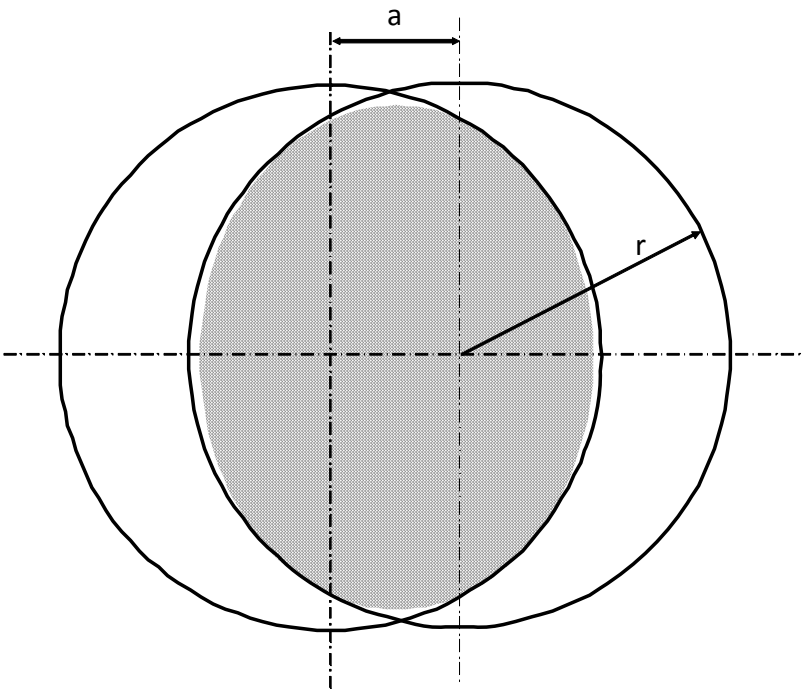

Figure 7(c). Schematic diagram of the geometries of the effective receiving area of the transducer. Cross-hatched area indicates the effective receiving area.

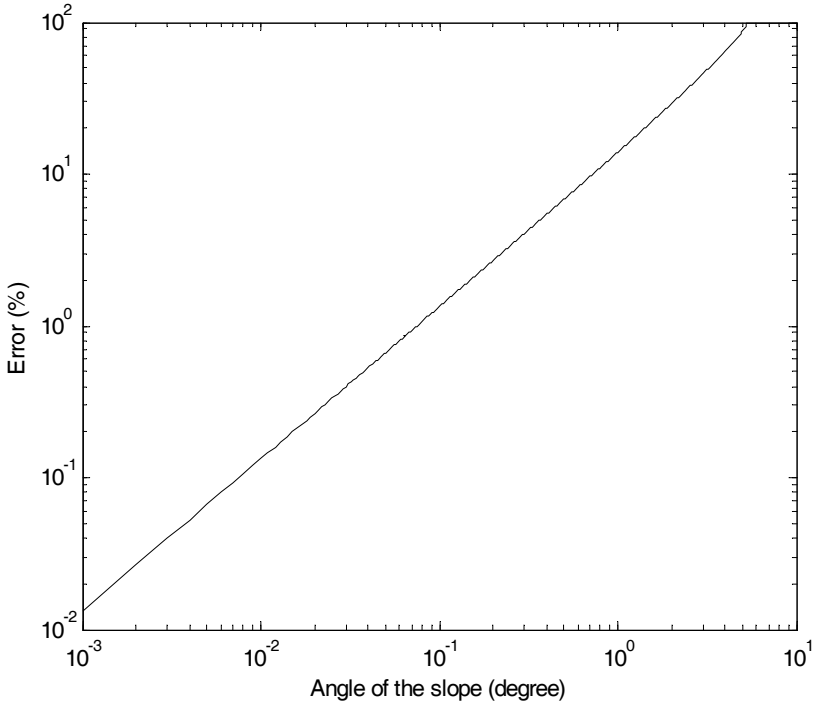

Figure 7(d). Reflection coefficient error caused by the surface slope of the lubricant contact area.

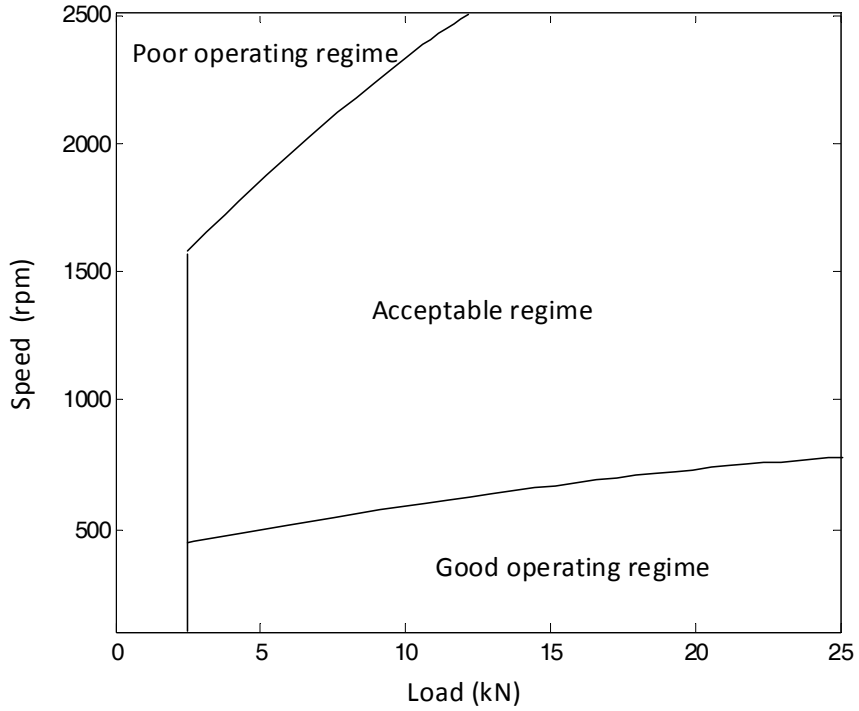

Figure 8. Limits of operation for lubricant-thickness measurement.

TABLES

Table 1. Transducer characteristics and dimensions.

Centre frequency f_c(MHz)	Wavelength in water at F_c λ*(mm)*	Focal length F(mm)	Element radius of curvature D(mm)	Active element diameter d(mm)
50	120	23.0	25	5

Table 2. Acoustic properties of lubricating oil and steel.

	Density ρ (kg/m^3)	Longitudinal wave velocity c (m/s)	Bulk modulus B(GPa)

Oil at 0.1 MPa	876	1460	1.84
Oil at 0.8 GPa	1002	3550	12.6
Oil at 1.5 GPa	1044	4500	21.2
Steel (EN24)	7900	5900	172

Table 3. Parameters required to calculate the theoretical lubricant-film thickness via the Dowson & Higginson equation [14].

Reduced modulus E'(GPa)	Reduced radius R'(m)	Pressure viscosity coefficient α (GPa^{-1})	Ellipticity parameter k	Simplified Elliptical Integrals ε	Effective viscosity η_0 (N/m^{2}s)
228	5.85e-3	20	11.5	3.8	0.2